Electronic Supplementary Material (ESI) for Sustainable Energy & Fuels.


# Plasmonic Au Nanoparticles Sandwiched $CuBi_2O_4/Sb_2S_3$ Photocathode with Multi-Mediated Electron Transfer for Efficient Solar Water Splitting

Mohit Kumar[1], Chandi Charan Ghosh[1], Bhagatram Meena[1], Tianyi Ma[2,*] Challapalli Subrahmanyam[1,*]

[1]Department of Chemistry, Indian Institute of Technology Hyderabad, Hyderabad, Telangana, 502285, India

[2]Centre for Translational Atomaterials, Swinburne University of Technology, John Street, Hawthorn, VIC 3122, Australia

[3]School of Science, RMIT University, Melbourne, VIC 3000, Australia

[*]Corresponding author:

Challapalli Subrahmanyam, Tel: +91-40-23016253, Email address: csubbu@iith.ac.in

Tianyi Ma, Email: tianyima@swin.edu.au

## 1.1 Materials and chemicals

Copper nitrate trihydrate($Cu(NO_3)_2.3H_2O$), Bismuth nitrate pentahydrate($Bi(NO_3)_3.5H_2O$), Chloroauric acid($HAuCl_4$), Antimony chloride($SbCl_3$), and FTO-coated glass($13\Omega\ sq^{-1}$) were purchased from Sigma Aldrich and used as received. Cetyltrimethylammonium bromide (CTAB) was purchased from Loba Chemie PVT. LTD. $AgNO_3$, $Na_2S_2O_3.3H_2O$ procured from Fisher Scientific. Ascorbic acid and anhydrous $Na_2SO_4$ were purchased from Avra Synthesis PVT. LTD.

## 1.2 Characterization

Crystal structure and phase identification of the as-prepared samples were examined by X-ray diffraction technique(XRD, Rigaku Pro, Cu Kα radiation λ = 1.5406 Å, 40kV, 200 mA) over a Bragg's angle of $20 \leq 2\theta \leq 70°$. The Field emission-scanning electron microscope (FE-SEM) (JEOL JSM 7800 FE-SEM) was used to characterize the morphological and compositional aspects of the samples. A transmission electron microscope(TEM) (JEOL F200) was used to measure the insights of the composite and crystalline morphology of the samples. High-resolution transmission microscopy(HRTEM) images, Scanning tunneling microscopic(STEM) micrographs, and selective area electron diffraction(SAED) tests were carried out at an acceleration voltage of 200 kV. The energy-dispersive X-ray mapping(EDX) was obtained on JEOL JSM 7800 FE-SEM. The UV-Vis absorption spectrum was acquired by a UV-Vis spectrophotometer (T90+, PG Instruments). The XPS scans were performed using an (AXIS Supra-Kratos analytical) spectrophotometer having a monochromatic X-ray source, Al Kα, of 1486.6 eV to measure the composition and oxidation state. The photoluminescence spectra of thin films were obtained from Horriba spectrophotometer to observe the recombination profile of the fabricated electrodes. IPCE measurements were done in Oriel IQE-200 in unbiased condition. Hydrogen gas was evaluated using a gas chromatograph(Mayura Analytical) equipped with a TCD detector.

## 1.3 Photoelectrochemical measurement

PEC measurements were performed in a three-electrode configuration using PGSTAT302N workstation(Metrohm instruments) for the with a Pt wire and saturated Ag/AgCl electrode as

counter electrode(CE) and reference electrode(RE), respectively. The working electrodes(WE) were having materials coated over FTO and these WE were illuminated with AM1.5 simulated solar light generated from a 150 W LED source, the incident light was calibrated to 100 $mW.cm^{-2}$. The photoelectrodes were illuminated from the front side with an area of 0.25 $cm^2$ exposed to illumination. Electrochemical impedance spectroscopy(EIS) measurements were performed at 0 V vs RHE with an AC amplitude of 5 mV and a frequency region from 0.1 Hz to 1 MHz in a 0.5 M $Na_2SO_4$ solution. $H_2SO_4$(pH=1) was used as an electrolyte for electrochemical measurements in acidic medium. All the potentials were converted to reversible hydrogen electrode (RHE) scale using the following equation:

$$E(V \text{ vs RHE}) = E(V \text{ vs Ag/AgCl}) + 0.197 + 0.059 \text{ pH}$$

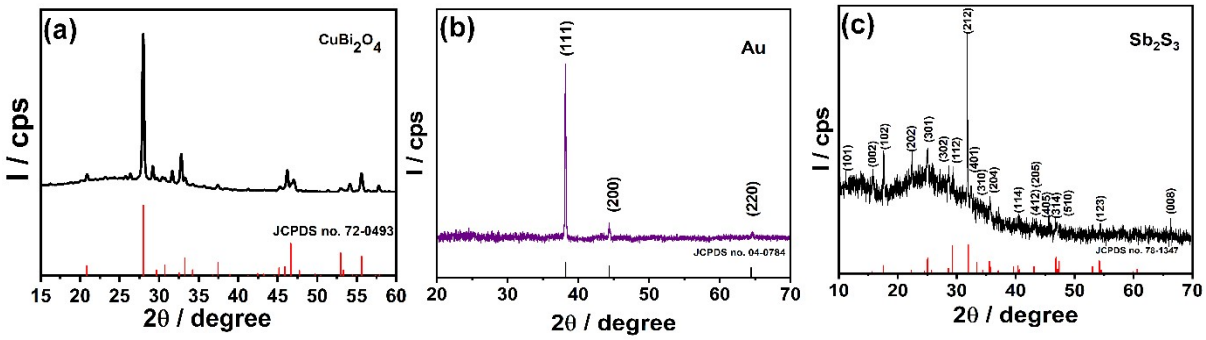


**Fig.S1** (a) XRD pattern of $CuBi_2O_4$ film with JCPDS #72-0493. (b) PXRD pattern of Au NPs with JCPD #04-0784. (c) XRD pattern of $Sb_2S_3$ with JCPDS #78-1347.

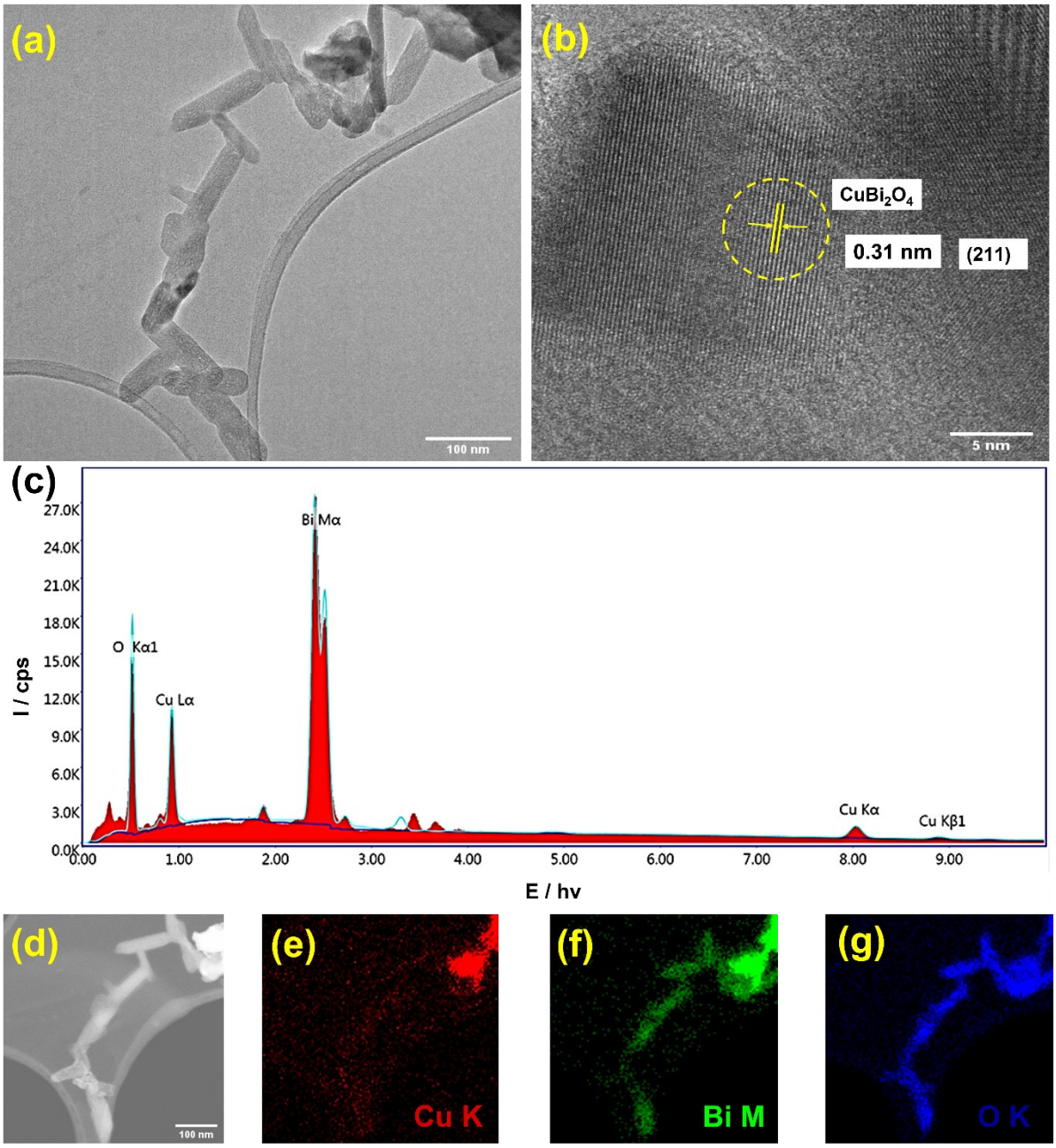


**Fig.S2** TEM micrograph of (a) $CuBi_2O_4$; (b) HRTEM image of $CuBi_2O_4$ (c)EDS elemental spectrum; (d) STEM image of $CuBi_2O_4$ rods; (e-g) Elemental analysis of Cu, Bi and O, respectively.

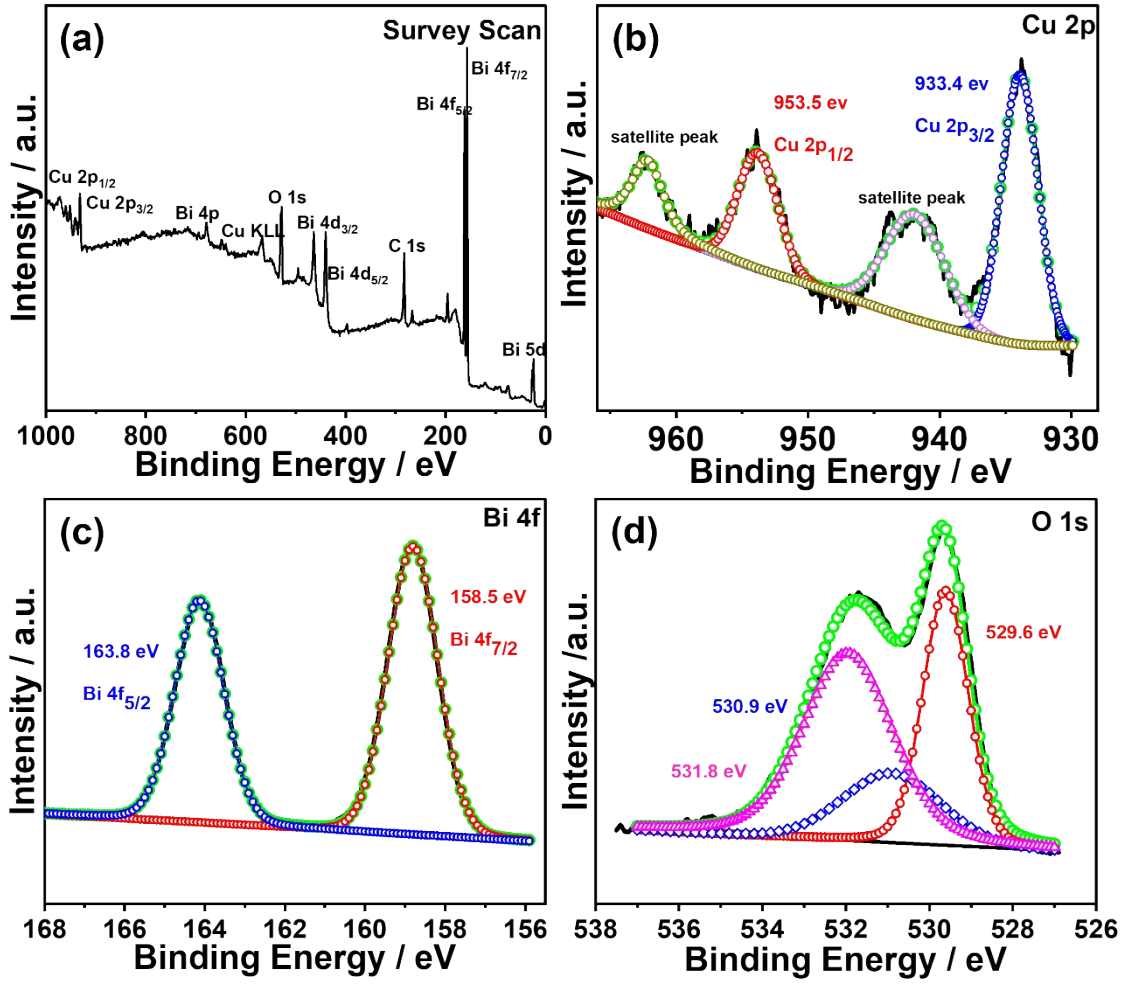


**Fig.S 3** $CuBi_2O_4$ XPS spectra (a) Survey scan and, high resolution spectrum of (b) Cu 2p; (c) Bi 4f; (d) O 1s.

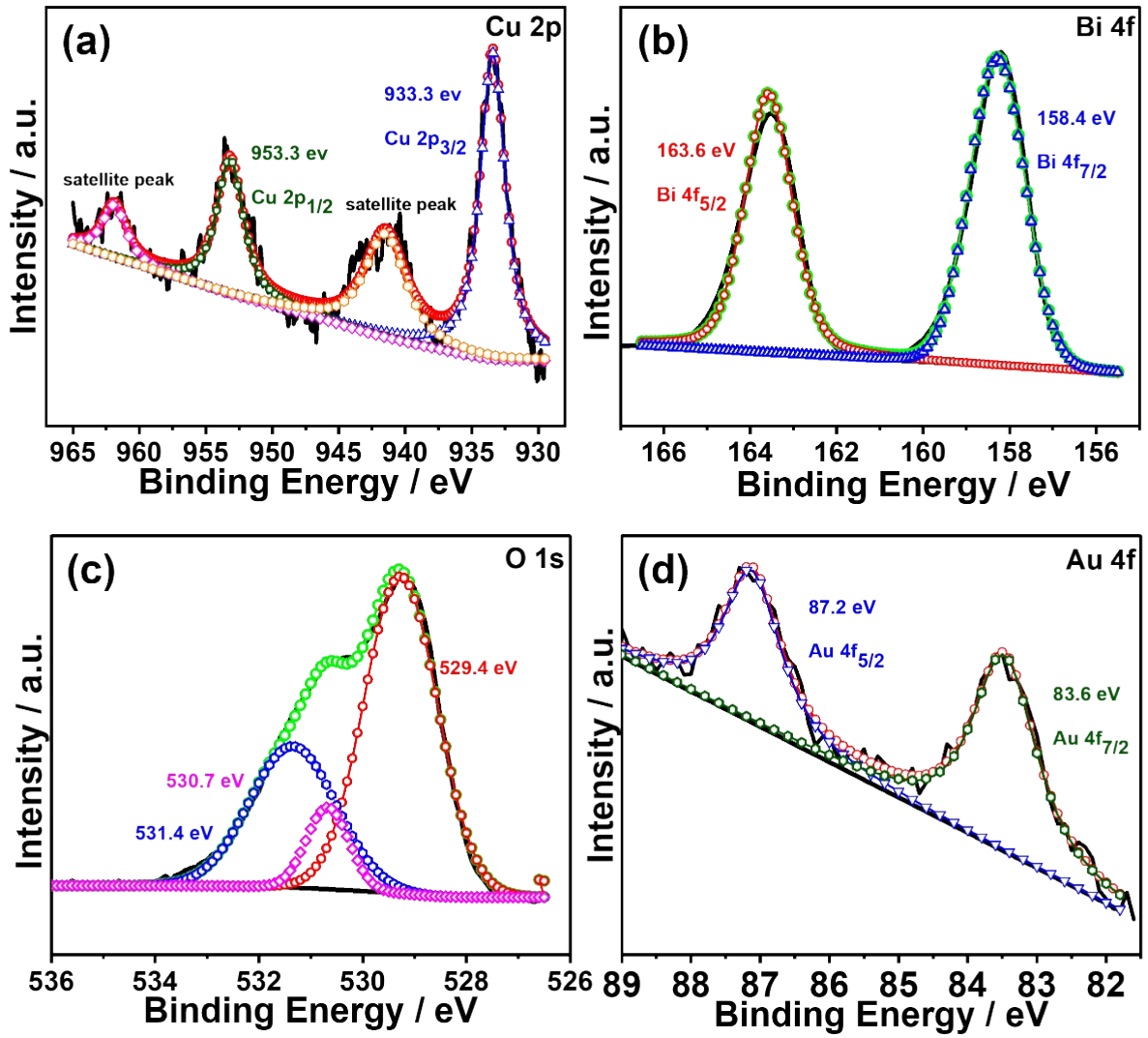


**Fig.S4** $CuBi_2O_4$/Au composite high resolution XPS spectrum of (a) Cu 2p; (b) Bi 4f; (c) O 1s; (d) Au 4f.

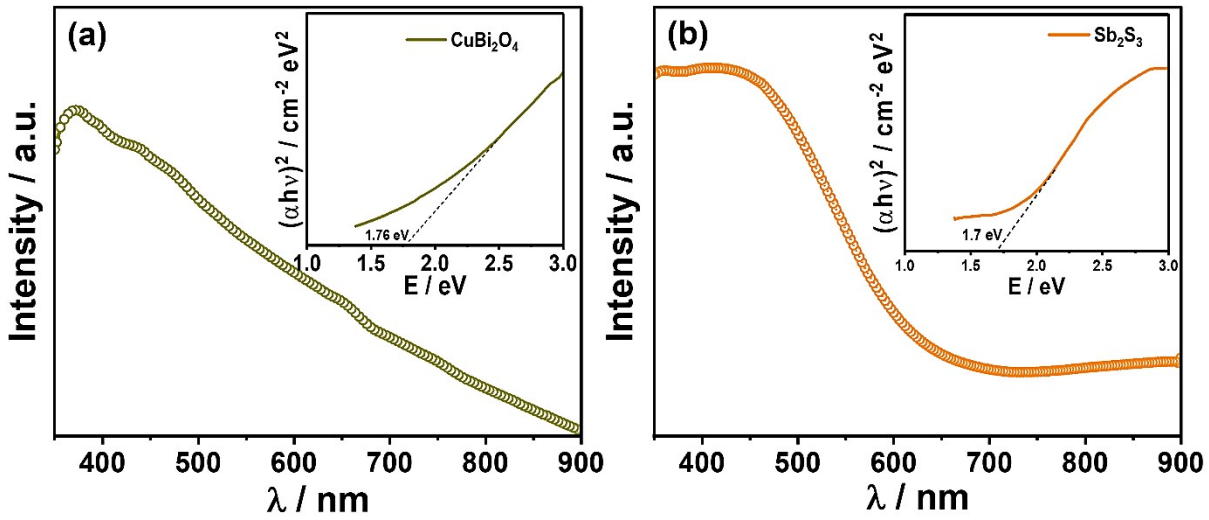


**Fig.S5** UV-Vis spectrum of (a) $CuBi_2O_4$ with Tauc's plot(inset) with bandgap 1.76 eV; (b) $Sb_2S_3$ with Tauc's plot(inset) with bandgap 1.7 eV.

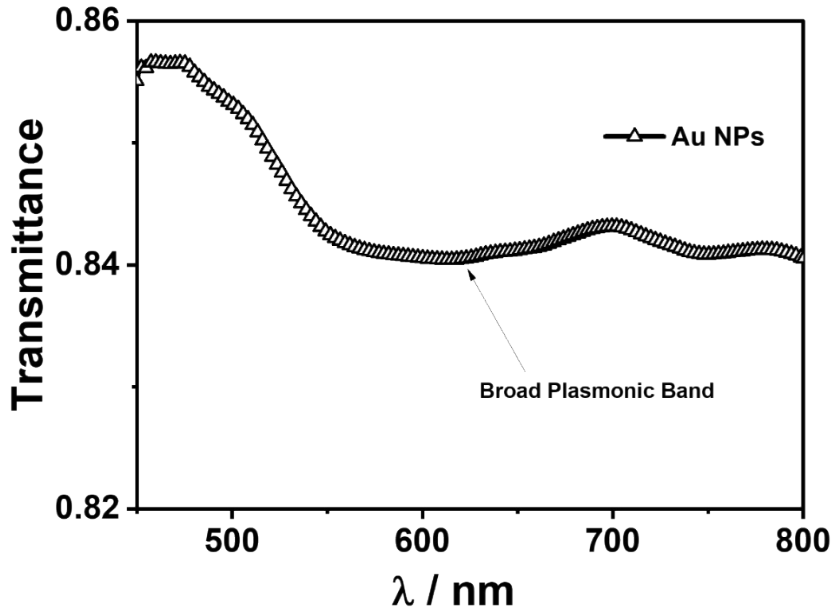


**Fig.S6** Transmittance spectra of thin gold film coated over glass slide

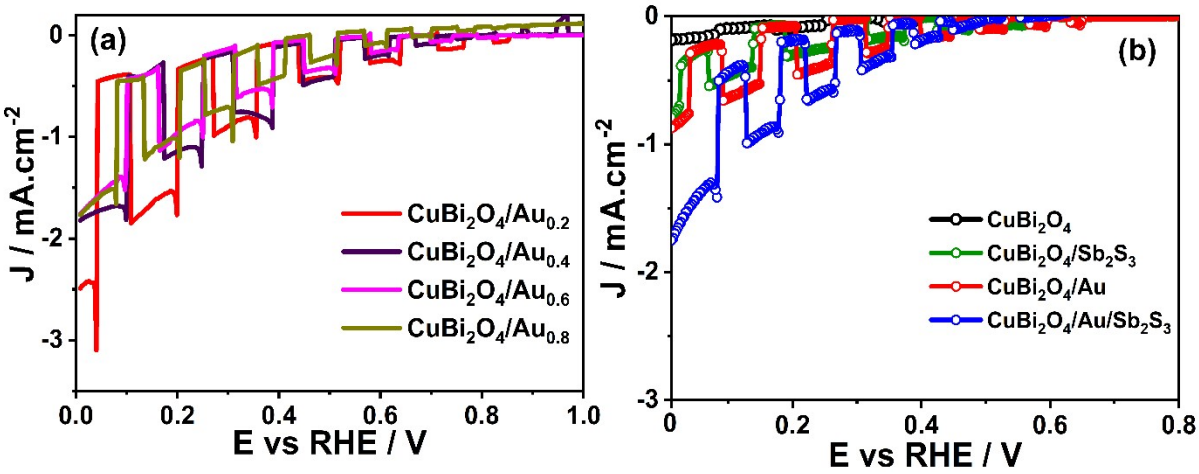


**Fig.S7** Linear sweep voltammetry curves for the (a) $CuBi_2O_4/Au_{0.2}$, $CuBi_2O_4/Au_{0.4}$, $CuBi_2O_4/Au_{0.6}$, and $CuBi_2O_4/Au_{0.8}$ photoelectrodes in neutral electrolyte. (b) $CuBi_2O_4$, $CuBi_2O_4/Sb_2S_3$, $CuBi_2O_4/Au$ and $CuBi_2O_4/Au/Sb_2S_3$ photoelectrodes in $H_2SO_4$(pH=1).

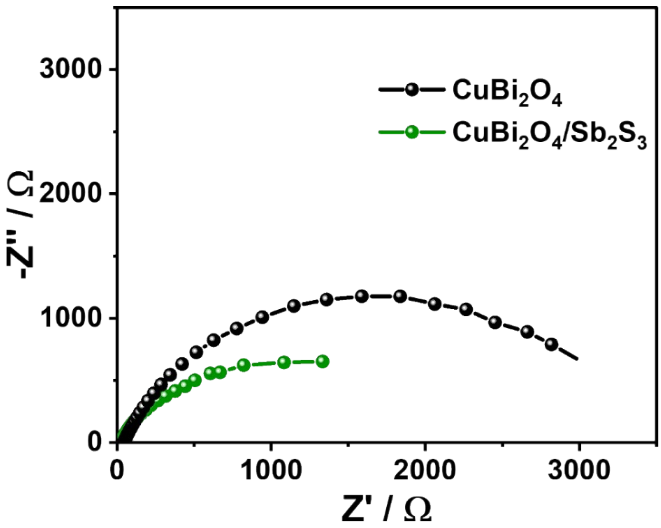


**Fig.S8** Impedance spectra of $CuBi_2O_4$, $CuBi_2O_4/Sb_2S_3$ photoelectrodes in 0.5 M $Na_2SO_4$ under illumination.

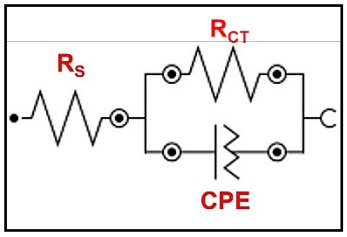


**Fig.S9** Equivalent Circuit for the Nyquist plots of $CuBi_2O_4$, $CuBi_2O_4/Au$ and $CuBi_2O_4/Au/Sb_2S_3$.

**Table S1.** Electrochemical impedance data fitting parameters of the pristine CIS, CIS/CdS, and CIS/CdS/$MoS_2$ photocathodes

| S. No. | Sample | $R_s(\Omega)$ | $R_{CT}$ (k$\Omega$) | CPE (m$\Omega^{-1}$) |
|---|---|---|---|---|
| 1. | **$CuBi_2O_4$** | 42.5 | 3.14 | 0.134 |
| 2. | **$CuBi_2O_4$/Au** | 39 | 2.54 | 0.078 |
| 3. | **$CuBi_2O_4$/Au/$Sb_2S_3$** | 41.5 | 0.347 | 1.17 |

**Table S2.** Summary for recently published reports for $CuBi_2O_4$ as photocathodic material for solar water splitting

| S. No. | Photocathode configuration | Electrolyte | \| J \| mA.cm$^{-2}$ | Onset $V_{RHE}$ | Stability | Light | Ref. |
|---|---|---|---|---|---|---|---|
| 1 | $CuBi_2O_4/MoS_2$ | 0.1M NaOH pH=12.5 | 0.182 at 0.6 $V_{RHE}$ | 0.9 | 200s | AM 1.5G | 1 |
| 2 | $CuO/CuBi_2O_4$/Pt | 0.3M $K_2SO_4$, 0.1M Phosphate buffer pH=6.8 | 0.72 at 0 $V_{RHE}$ | - | 600s | AM 1.5G | 2 |
| 3 | $CuBi_2O_4$/Ag-$CuBi_2O_4$/Pt | 0.1M NaOH pH=12.8 | 0.6 at 0.5 $V_{RHE}$ | 1.1 | 30 m | AM 1.5G | 3 |
| 4 | $CuBi_2O_4$/Au/N,Cu−C | 0.3 M K2SO4/0.2 M phosphate buffer (pH 6.68) | 0.31 at 0.5 $V_{RHE}$ | - | 3000s | AM 1.5G | 4 |
| 5 | CBO/ZnSe/P25 | 0.3 M $K_2SO_4$/0.2 M phosphate buffer (pH=6.65) | 0.43 at 0.3 $V_{RHE}$ | - | 5000s | 300 W Xe lamp | 5 |
| 6 | CBO/NiO/$SrTiO_3$ | 0.1M KPi buffer | 0.4 at 0 $V_{RHE}$ | - | 3h | AM 1.5G | 6 |

| | | | | | | | |
|---|---|---|---|---|---|---|---|
| 7 | $CuBi_2O_4$ | 0.3 M K2SO4/0.2 M phosphate buffer (pH 6.65) with $H_2O_2$ | 2.66 at 0.6 $V_{RHE}$ | > 1.0 | | AM 1.5G | 7 |
| 8 | $O_v$/CBO/Zn-CBO | 0.3 M K2SO4/0.2 M phosphate buffer (pH 6.65) | 0.6 at 0.3 $V_{RHE}$ | 1 | 300s | 300 W Xe lamp | 8 |
| 9 | CuO/CBO | 0.5M $Na_2SO_4$ solution (pH= 7) | 0.9 at 0.1 $V_{RHE}$ | 1 | 75% retention up to 2500s | 250 W Xe lamp | 9 |
| 10 | FTO/Au/CBO/Pt | 0.1M $Na_2SO_4$ (pH = 6.8) | 1.24 at 0.1 $V_{RHE}$ | - | 3000s | 300 W Xe lamp | 10 |
| 11 | FTO/Textured CBO | 1M NaOH (pH = 13.6) | 1.77 at 0.4 $V_{RHE}$ | 1 | 40s | AM 1.5G | 11 |
| 12 | FTO/Textured CBO | 0.1M $Na_2SO_4$ (pH= 6.8) | 0.72 at -0.6 $V_{Ag/AgCl}$ | 1 | 40s | AM 1.5G | 11 |
| 13 | CBO/Au/Sb2S3 | 0.5 M $Na_2SO_4$ (pH = 6.65) | 3.2 at 0 $V_{RHE}$ | 1 | 7200s | AM 1.5G | **This work** |
| 14 | CBO/$Sb_2S_3$ | 0.5 M $Na_2SO_4$ (pH = 6.65) | 2.2 at 0 V vs RHE | 1 | 7200s | AM 1.5G | **This work** |
| *Note: Some values were roughly read from the corresponding given graphs | | | | | | | |

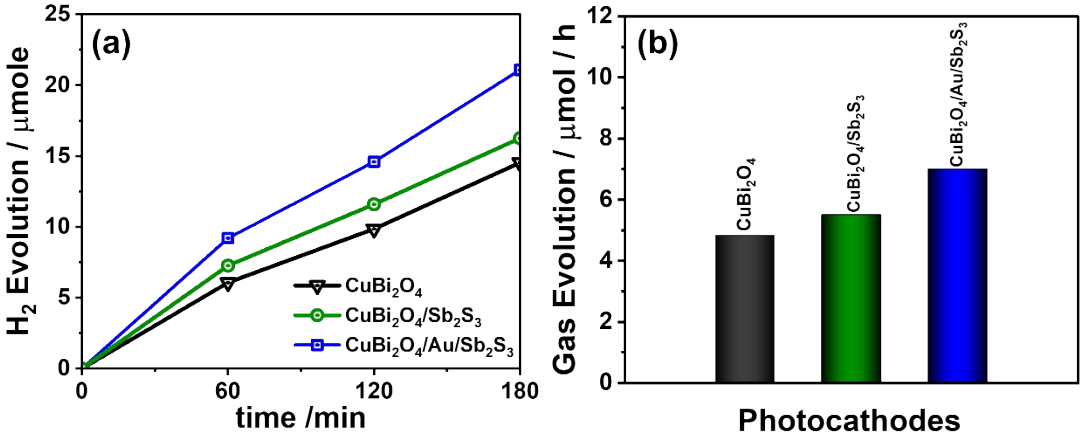


**Fig.S10** (a) $H_2$ evolution from the $CuBi_2O_4$, $CuBi_2O_4$/ $Sb_2S_3$ and $CuBi_2O_4$/Au/$Sb_2S_3$ photocathodes; (b) rate of $H_2$ evolution from the $CuBi_2O_4$, $CuBi_2O_4$/ $Sb_2S_3$ and $CuBi_2O_4$/Au/$Sb_2S_3$ photocathodes.

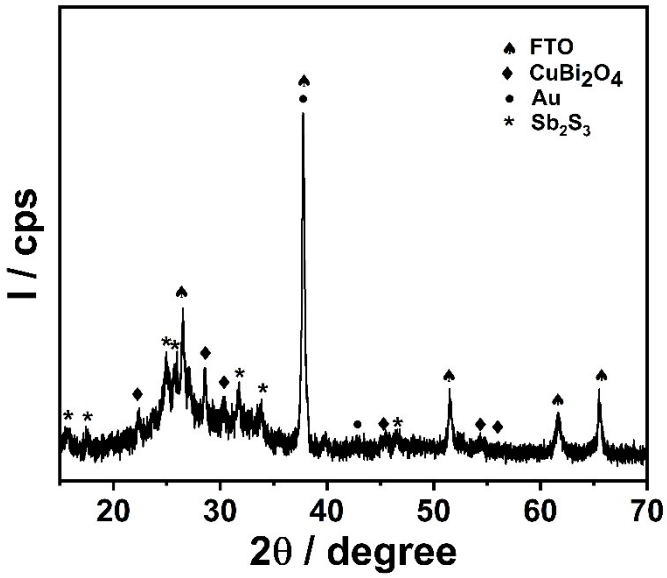


**Fig.S11** PXRD pattern of the $CuBi_2O_4$/Au/$Sb_2S_3$ photoelectrode after PEC test in neutral electrolyte.

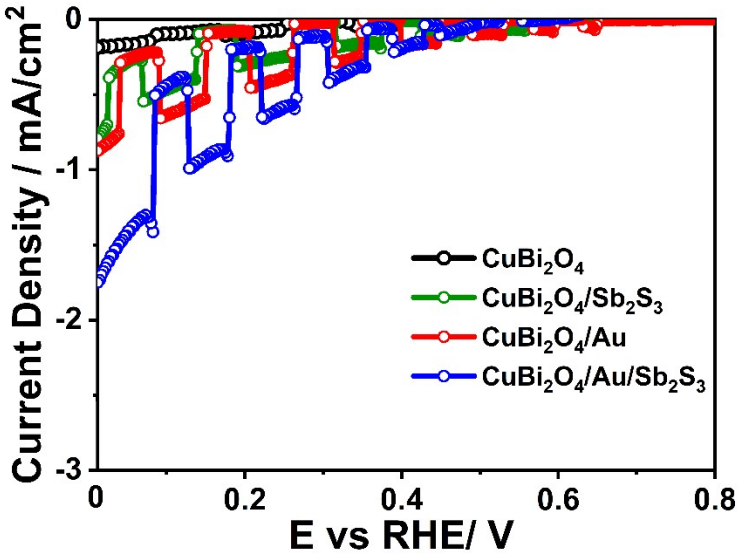


**Fig.S12** Photocurrent density-voltage(J-V) curves of $CuBi_2O_4$, $CuBi_2O_4/Sb_2S_3$, $CuBi_2O_4$/Au and $CuBi_2O_4$/Au/$Sb_2S_3$ photoelectrodes in $H_2SO_4$(pH=1).

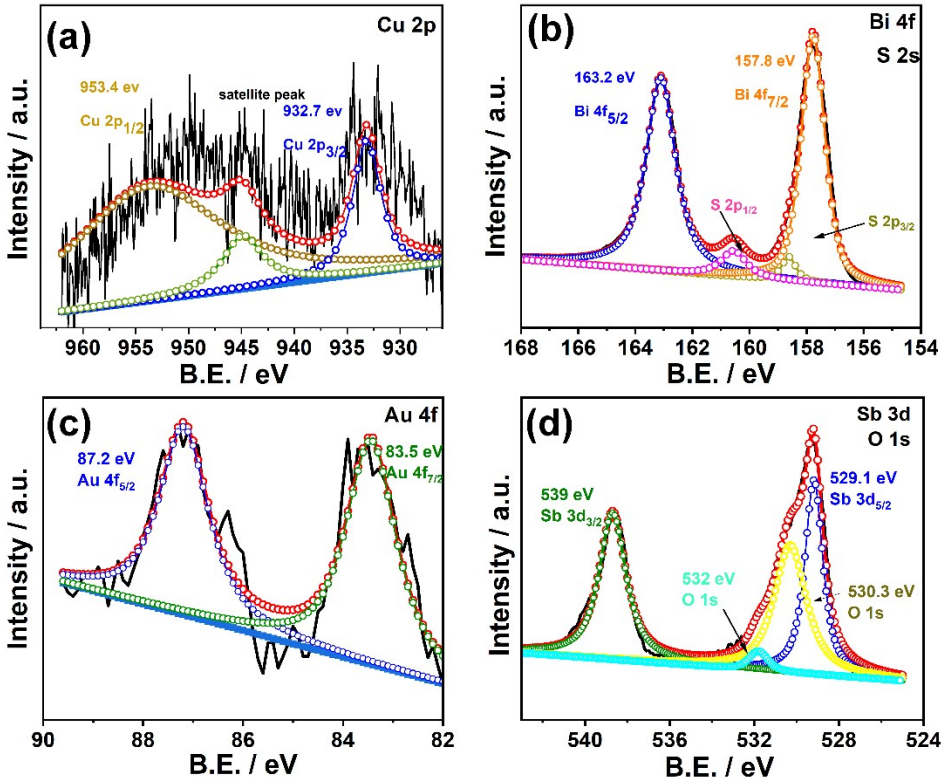


**Fig.S13** XPS spectrum of $CuBi_2O_4/Au/Sb_2S_3$ composite (a) Cu 2p; (b) Bi 4f & S 2s; (c) Au 4f; (d) Sb 3d & O 1s.

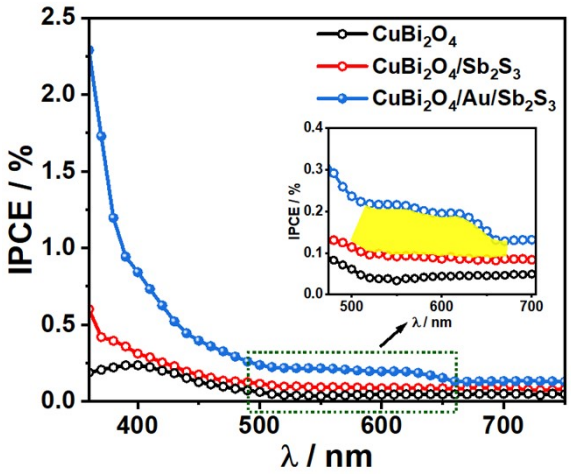


**Fig.S14** IPCE spectra of the photoelectrodes in unbiased condition[12].

## References


1 K. Varunkumar and R. Sellappan, *Mater. Chem. Phys.*, 2021, **261**, 124245.

2 H. S. Park, C. Y. Lee and E. Reisner, *Phys. Chem. Chem. Phys.*, 2014, **16**, 22462–22465.

3 D. Kang, J. C. Hill, Y. Park and K. S. Choi, *Chem. Mater.*, 2016, **28**, 4331–4340.

4 N. Xu, F. Li, L. Gao, H. Hu, Y. Hu, X. Long, J. Ma and J. Jin, *ACS Sustain. Chem. Eng.*, 2018, **6**, 7257–7264.

5 S. Wei, N. Xu, F. Li, X. Long, Y. Hu, L. Gao, C. Wang, S. Li, J. Ma and J. Jin, *ChemElectroChem*, 2019, **6**, 3367–3374.

6 J. Lee, H. Yoon, K. S. Choi, S. Kim, S. Seo, J. Song, B. U. Choi, J. Ryu, S. Ryu, J. Oh, C. Jeon and S. Lee, *Small*, 2020, **16**, 1–11.

7 Y. Xu, J. Jian, F. Li, W. Liu, L. Jia and H. Wang, *J. Mater. Chem. A*, 2019, **7**, 21997–22004.

8 S. Wei, C. Wang, X. Long, T. Wang, P. Wang, M. Zhang, S. Li, J. Ma, J. Jin and L. Wu, *Nanoscale*, 2020, **12**, 15193–15200.

9 S. Pulipaka, N. Boni, G. Ummethala and P. Meduri, *J. Catal.*, 2020, **387**, 17–27.

10 D. Cao, N. Nasori, Z. Wang, Y. Mi, L. Wen, Y. Yang, S. Qu, Z. Wang and Y. Lei, *J. Mater. Chem. A*, 2016, **4**, 8995–9001.

11 J. Li, M. Griep, Y. Choi and D. Chu, *Chem. Commun.*, 2018, **54**, 3331–3334.

12 J. Li, S. K. Cushing, P. Zheng, T. Senty, F. Meng, A. D. Bristow, A. Manivannan and N. Wu, *J. Am. Chem. Soc.*, 2014, **136**, 8438–8449.